35th AIAA Plasmadynamics and Lasers Conference
28 June - 1 July 2004, Portland, Oregon

AIAA 2004-2738

Stall control at high angle of attack with periodically excited EHD actuators

Roberto Sosa [*] ,

Laboratorio de Fluidodinámica, Universidad de Buenos Aires, Buenos Aires, 1406, Argentina.

Eric Moreau.[†], Gérard Touchard [‡]
Laboratoire d'Etudes Aerodynamiques (UMR 6609 CNRS), Université of Poitiers, Poitiers, 86022, France.

and

Guillermo Artana[§]
Laboratorio de Fluidodinámica, Universidad de Buenos Aires, CONICET , Buenos Aires,1406, Argentina.

We analyze the modifications of the flow around a NACA 0015 airfoil when the flow is periodically perturbed with an electrohydrodynamic (EHD) actuator. The device used consists of two bare electrodes flush mounted on the surface of the profile operated in a discharge regime characterized by the formation of a plasma sheet contouring the body. In this study, we analyze the influence of the frequency of a periodic actuation on the aerodynamic performance of the airfoil. The analysis is undertaken with measurements of the surface pressure distribution and of the flow fields with Particle Image Velocimetry technique. The experiments indicate that at moderate Reynolds numbers (150000<Re<333000), the actuation enables a reattachment of the flow at high values of the angle of attack (α>15°).

Nomenclature

b	=	thickness of the airfoil
c	=	cord length
f_{exc}	=	frequency of excitation of the actuator
l	=	curvilinear coordinate in the tangential direction of the surface
C_μ	=	momentum addition coefficient
Cw	=	power addition coefficient
Cp	=	surface pressure coefficient
C_{Dp}	=	pressure drag coefficient
C_l	=	lift coefficient
F^+	=	reduced frequency of excitation
L_{ele}	=	electrode length in the spanwise direction
P_i	=	surface pressure at position i

[*] PhD Student, Department Mechnical Engineering, Paseo Colón 850, Ciudad de Buenos Aires, Argentina
[†] Maitre de Conferences, Bvd. Pierre et Marie Curie, Futuroscope Cedex, France.
[‡] Professor, Bvd Pierre et Marie Curie, Futuroscope Cedex, France.
[§] Professor, Department Mechanical Engineering, Paseo Colón 850, Ciudad de Buenos Aires, Argentina. (gartana@fi.uba.ar)

Re = Reynolds number= $\frac{U_0\, c}{\upsilon}$
U_0 = free stream velocity
W = Electric Power of the discharge
α = angle of attack
δ = length of the interelectrode space in the streamwise direction
ρ = air density
τ_{el} = electric force per unit area
υ = kinematic coefficient of viscosity of the air

I. Introduction

Electrohydrodynamic Actuators

Actuators are devices that add momentum to a flow with the objective of modifying its characteristics. The electrohydrodynamic (EHD) actuators produce a weakly ionized gas and add momentum to the flow by the collisions of charged particles with the neutral species. Their name is based on the fact that currents involved are so low that the intensities of the magnetic forces are negligible compared to the electric ones.

The main advantages of these actuators are that they have no moving part, a very short response time (delays in the establishment of a discharge are theoretically of the order of nanoseconds) and a relative good efficiency to transform electrical to mechanical energy[1].

EHD actuators may be divided in three large groups
-coronas based devices
-dielectric barrier discharge devices
-plasma sheet devices

Coronas based devices use a self sustaining discharge accompanied by a strong inhomogeneity of the electric field configuration. They comprise the use of at least one electrode having a very low radius of curvature that generally is a needle or a very thin wire.

The electric field configuration confines the ionization process to regions close to the high-field electrodes. Thus, in this phenomenon there are active electrodes, surrounded by ionization regions where free charges are created and low-field regions where charged particles drift and react in their movement towards the passive electrodes. These kinds of actuators may be effective to modify different flows [2-5], but in general require a large power consumption compared to other EHD actuators.

The devices with dielectric barrier use periodically excited electrodes, one exposed to the air while the other is encapsulated by a dielectric material [6-7] . The dielectric barrier interposed between both electrodes serves to stabilize the discharge avoiding the impact of the ions on the cathode and thus preventing the heating of it and the formation of new avalanches or breakdown from the electron secondary emission. Usual configurations consist on planar electrodes separated by a thin dielectric film and in an arrangement parallel in the spanwise direction of an aerodynamic surface. Excitations are in general in the range of some kHz and a diffuse light indicating an ionization process occurs at close vicinity of the air exposed electrode.

Plasma sheet devices use both electrodes air exposed. They are disposed flush mounted on the surface of a dielectric body with an interelectrode distance of some centimeters. The electrodes may be excited with a DC or with a periodic potential difference. The stabilization of the discharge is achieved by means of a careful finishing of electrodes (to impede the formation of spurious electric field concentration) and by means of the airflow that inhibit thermal instabilities that could lead to filamentation or arcs [8]. The device produces a homogeneous luminescence that occupies the whole interelectrode space along the span and in this region the surface looks contoured by a thin film of ionized air.

Periodic excitation of flows with separation

The separation of boundary layers in the case of aerodynamic bodies produces energy and lift losses. Consequently the use of actuators in this area has focused on the alteration of the location of the boundary layer separation and the mitigation of the effects produced by it.

In flow around airfoils, the main objectives of the research efforts with actuators have been to prevent or to postpone the stall using either steady or unsteady actuations.

When using a steady actuation in the flow, the purpose of the actuation is to impart additional momentum to the retarded fluid within the boundary layer and thus to delay separation.

When dynamic actuations are proposed, a periodic momentum addition is imposed to fluid layers close to the airfoil surface. The flow receptivity to excitations related to the fluid inherent instabilities[9], (specially those associated to the separated shear layer of the Kelvin-Helmholtz type) is taken into account when performing the cyclic actuation. The purpose is to profit the natural amplification of small periodic perturbations and by this mean promoting the entrainment of high speed fluid of the freestream into the regions of the low velocities separated flow.

Several kind of actuators including, internally mounted devices (speakers/acoustic drivers, pistons, oscillatory-flow valve systems or piezoelectric based diaphragms) and surface mounted devices (ribbons, fliperons, piezo-based benders and electromagnetic force actuators) have been tested and are summarized in a recent thorough review[10].

Independently of the type of actuator employed, the optimal location seems to be close to the separation line (point)[10], and at a fixed level of excitation the periodic excitation results energetically more efficient than the steady one[11].

The effect of the frequency of actuation (f_{exc}) on the flow has been studied in terms of a reduced frequency F^+

$$F^+ = \frac{f_{exc}\, c}{U_0}$$

(with c the cord length and U_0 the velocity of the free stream). Empirically found the range of optimum frequencies F^+ was close to the unity, a value quite close to the unstable frequencies of the separated shear layer. Concomitantly it has been reported that for the range of high reduced frequencies F^+ the actuation becomes much less effective[10].

Objectives of this work

The first researches proposing stall control with dielectric barrier devices [12-15] or with plasma sheet actuators [16-19] have been mainly concerned with steady excitation of the flow. A very recent report has described experiments on oscillating airfoils with dielectric barrier devices considering unsteady excitations [20].

We propose in this work to analyze the influence of the frequency of excitation on the improvement of aerodynamic performances with plasma sheet devices that periodically perturb the flow. Our study is based on the analysis of flow fields obtained by Particle Image Velocimetry technique and on surface pressure distributions.

In order to facilitate the comparisons of the aerodynamic performance achieved with the EHD actuation with other kind of actuations we have selected the NACA0015 airfoil model that has been extensively studied by other researchers [10, 21-22] using dynamic excitation.

II. Experimental Setup

A. Wind tunnel and models

The measurements have been done in a wind tunnel loop of the Laboratoire d'Etudes Aerodynamiques. The tunnel has a rectangular cross section (0.50 x 0.50 m^2) and enables testing at flow velocities up to 30m/s. The airfoil model was a NACA 0015 section shape of Polymethyl metacrylate (PMMA) (Figure1). The chord dimension was 200 mm and the spanwise dimension was 450 mm. The airfoil has been fabricated in two separate parts (male and female) enabling to obtain a hollowed body. The fixation of the airfoil was performed on both ends through pieces of electrical insulating material (Nylon). In the test section, the angle of attack was manually varied and recorded in digital photographs to establish its value with an accuracy upto 0.1°.

Detailed descriptions of the wind tunnel characteristics and of the models may be found in a previous report [23]. Experiments have been undertaken in a velocity range of 10-25 m/s with an associated Reynolds number ($Re=U_0\, c/\nu$) comprised in the interval $1.3\ 10^5<Re<3.3\ 10^5$. The airfoil was disposed with different angles of attack corresponding to the poststall regimes. At the flow conditions of our experiments, separation with no reattachment and without hysteresis was observed for angles higher than 15º. The blockage ratio in the wind tunnel loop reached in the worst condition 8.6 at the highest angle of attack (21.7°). No correction for blockage effects has been applied to the data obtained.

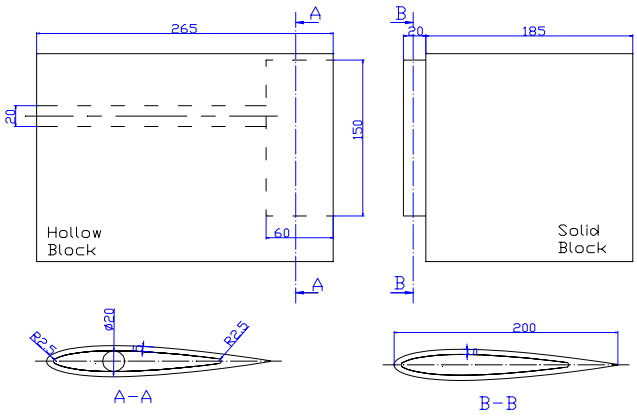

Figure 1: Scheme of the NACA0015 Airfoil Model.
Model in PMMA

B. EHD excitation

Two plane parallel electrodes, consisting on strips of 3.5mm width of thin aluminum foil (50µm thick), were flush mounted on the surface of the airfoil in the spanwise direction covering 85 % of the span. One of them was located at the leading edge position (x/c=0) while the second one was at disposed at x/c=0.18 on the suction side of the airfoil. The ends of both electrodes were rounded to avoid a large field concentration in this region.

A high voltage power amplifier (0 to ±20 kV, ±20 mA , 20kHz bandwidth) and a signal generator were used to impose a positive high voltage (H.V.) step function in the leading edge electrode while the potential of the downstream electrode was imposed by a negative DC high voltage power supply (-40kV, 3.75 mA). A H.V. probe enabled the monitoring of the signal delivered by the sources.

The discharge current was measured with the help of an AC current transformer (20 mA, precision lower than 3 µA, bandwidth of 10 kHz) connected to an oscilloscope. The current transformer was of the inductive type and consisted of a toroidal sensor with inner diameter of 28 mm placed around the A.C. H.V. cable.

Power and Momentum addition to the flow

The power added to the flow as a consequence of actuation may be expressed by means of a non dimensional power coefficient C_W defined as

$$C_W = \frac{W}{L_{ele}} \frac{1}{0.5\,\rho\,U_0^3 b} \frac{\delta}{c}$$

δ is the interelectrode distance, L_{ele} is the electrode length and b is the thickness of the airfoil. In our case W is the electric power of the discharge and may be easily calculated based on the discharge current and the voltage difference of the electrodes.

Other researchers[10] have preferred an analysis based on a momentum addition coefficients which for our actuator may be expressed by mean of a non dimensional parameter C_μ defined as

$$C_\mu = \frac{\tau_{el}\ \delta}{0.5\,\rho\,U_0^2\quad c}$$

where τ_{el} is the electric force per unit area produced by the discharge. Previous research[1] undertaken with steady actuations on flows around a flat plate has indicated that τ_{el} is a function of the velocity of the airtsream over the discharge and, that typical values of C_μ are about 0.015. These estimations have been done assuming that the alterations of fluid properties by ionization of the gas were negligible. In this work we prefer to undertake our analysis with C_W.

C. Velocity field measurements

The velocity field has been measured using a Particle Image Velocimetry (PIV) technique. The tracers have been originated by a smoke generator producing droplets of a pure cosmetic grade oil with a mean size of about 0.3 μm. The system was illuminated with a laser sheet of a Yag laser of 200mJ. Each pulse had a duration of 0.01 microseconds and the time between a pair of pulses was, depending on the experiment, in the range of 20-50 microseconds. A progressive scan interline camera capable of producing images of 1280 × 1024 pixels was used.

PIV data processing

To obtain the vector fields a treatment of the recorded images was undertaken with commercial PIV software providing an adaptive correlation technique. In this treatment we have considered 2 refinements steps and the final interrogation area size was of 16x16 pixels[2] with an overlap of 50%.

Each velocity field was filtered with both, a peak-validation and a range validation filters. Peak validation filter based on a detectability criterion[24] that validated vectors with a ratio of the highest peak to the second highest peak in the correlation plane larger than a fixed value (1.2 in our case). The range validation filter enabled the establishment of the range admitted for the modulus of the velocity vectors. In our case, we have considered a value of 3 times of the flow velocity U_0 as the upper limit.

Six hundreds pairs of digital images taken at pairs every 0.1s were examined in each experiment. The mean velocity field of the airflow was obtained by averaging the six hundred instantaneous flow fields. Convergence of the time averaged values towards the mean value has been tested adopting lower intervals and is largely assured with our experimental conditions.

Particle tracking

In PIV experiments the velocity of the tracers and that of the fluid particles surrounding them should be coincident. The occurrence of slipping causes the seeding particles to "swim" in the moving media and the information obtained must then be carefully examined. In our experimental design, in as much as the operation of the smoke generator created a cloud with a mean particle diameter of 0.3μm the influence of coulombian forces on tracers trajectories can be disregarded without introducing a significant error, as concluded in our previous report [25].

Uncertainty of flow field measurements

The system resolution for distances can be estimated as the product of the pixel resolution (a very conservative values is 1/4 pix) and the pixel size. In that way, the resolution of the velocity field can be estimated dividing the latter value by the time between the pair of pulses. In our case the pixel size (*ps*) varied from about 0.09-0.2 (10^{-3} m/pixel) leading to a very conservative value of uncertainty for the velocity of

$$\Delta v \le \frac{1}{4}(pixel)\cdot ps(m/pixel)\frac{1}{\Delta t(\sec)} \cong 1.125\, m/s$$

D. Pressure measurements

For the surface pressure distribution experiments, 30 pressure ports drilled at the half of the span location of the airfoil were considered. The pressure tapping hole diameters were of 1.5 mm and their centers were streamwise spaced as described in table I. A tubulation with electrical insulating tubes of Tygon (internal diameter= 0.5mm) carried the pressure from the ports to a set of 30 independent solid state sensors (ion-implanted piezoresistive strain gage) with their output connected to a data acquisition system. The tubings were inserted in the holes, passed through the hollow of the airfoil and brought out through the support of one end of the model.

The free stream velocity U_0 was measured using a micromanometer connected to a Pitot tube positioned at the entrance of the test section. The static pressure corresponding of this device was also used as a reference pressure P_0 of the free air stream.

In this work we make use of a coefficient Cp defined as

$$Cp = \frac{P_i - P_0}{\frac{\rho U_0^2}{2}}$$

being the surface pressure P_i at station i and ρ the gas density.

The lift and of drag pressure coefficients

The coefficients of lift and drag pressure are estimated by integration of the C_p distribution around the airfoil.

$$C_l(t,\alpha) = \frac{1}{c}\oint C_p(s,t,\alpha)\frac{\vec{U}_0}{U_0} \times d\vec{l}$$

$$C_{Dp}(t,\alpha) = \frac{1}{c}\oint C_p(s,t,\alpha)\frac{\vec{U}_0}{U_0}.d\vec{l}$$

where l is the curvilinear coordinate in the tangential direction of the surface and α is the angle of attack of the airfoil.

Port Number	Intrados x/c	Extrados x/c
1	0.03	0.02
2	0.05	0.10
3	0.08	0.17
4	0.10	0.25
5	0.13	0.32
6	0.16	0.39
7	0.18	0.47
8	0.22	0.54
9	0.28	0.62
10	0.33	0.70
11	0.38	0.77
12	0.43	-
13	0.48	-
14	0.53	-
15	0.58	-
16	0.63	-
17	0.68	-
18	0.73	-
19	0.78	-

Table I: Pressure ports position.
Positions are expressed refereed to the cord length

When separation takes place, the surface pressure at different ports may exhibit a time dependent behavior. The pressure detected by the sensor is not the real surface pressure as this magnitude is dampened by the system of pressure transmission [26].

Therefore, to obtain the effective instantaneous value of the pressure a reconstruction of the signal is required. A way of achieving this is to establish the gain for the different frequencies of the tube-transducer system.

However, the mean value of the pressure may be easily obtained without any reconstruction by an adequate time integration of the direct measurement of the fluctuating surface pressure.

In order to assume the convergence to the mean value, the interval T of measurement must be much longer than the characteristic time of the flow fluctuations. In our case, the characteristic time may be roughly estimated[27] considering a Strouhal number about a value of 0.2. Our experiments have been performed by acquiring the surface pressure at times larger than seconds. Such lapses, even in the more adverse situations exceeded in more than one order of magnitude those characterizing the dynamics of vortex shedding.

The estimations of the time averaged value of Cp has also been carried out under the same considerations about the time of integration T than those for surface pressure

$$\overline{C}_p(s,\alpha) = \frac{1}{T}\int_0^T Cp(s,t,\alpha)dt$$

In next sections we make also use of the coefficients C_l (α) and C_{Dp}(α) defined by

$$C_l(\alpha) = \frac{1}{c}\oint \overline{C}_p(s,\alpha)\frac{\vec{U}_0}{U_0}\times d\vec{l}$$

$$C_{Dp}(\alpha) = \frac{1}{c}\oint \overline{C}_p(s,\alpha)\frac{\vec{U}_0}{U_0}.d\vec{l}$$

Uncertainty analysis

The equivalence between the coefficient $C_l(\alpha)$ and $\overline{C}_l(\alpha)$ the time averaged values of $C_l(t,\alpha)$

$$\overline{C}_l(\alpha) = \frac{1}{T}\int_0^T C_l(t,\alpha)dt$$

or between $C_{Dp}(\alpha)$ and $\overline{C}_{DP}(\alpha)$

$$\overline{C}_{DP}(\alpha) = \frac{1}{T}\int_0^T C_{Dp}(t,\alpha)dt$$

are assured only when a concordance of phase between the pressures values at the different measurement points is verified. Such concordance (temporal problem) was not tested in the present report.

Also as a consequence of the geometry of the model, there was a region towards the trailing edge (x/c >0.78) where it was not possible to dispose pressure probes and the pressure distribution there remained undetermined.

Owing to this spatial problem, the coefficients $C_l(\alpha)$ and $C_{Dp}(\alpha)$ could be calculated only with a integration over those coordinates that ignore the fluid dynamics of regions quite close to the trailing edges.

Although for these two reasons (spatial and temporal problems) it was not adequate to directly extrapolate values of the mean lift force and drag pressure force experienced by the airfoil from the parameters $C_l(\alpha)$ and $C_{Dp}(\alpha)$ of our tests, these coefficients gave a fruitful data and resulted a useful tool to compare the aerodynamic performance of the airfoil in the presence or absence of the discharge.

III. Experimental Results

A. Discharge Characteristics

The discharge of our experiments was produced with a periodic H.V. excitation of the anode and a simultaneous steady H.V. excitation of the cathode.

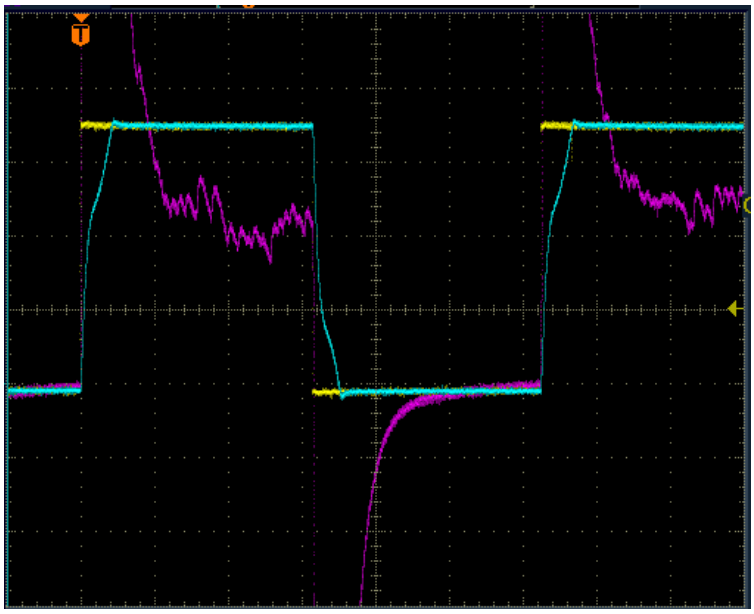

Figure 2: Discharge current and anode voltage potential waveform at f_{exc} 400Hz
In yellow: Driving Voltage, In light blue: H.V. signal(5 kV/div)In magenta: Discharge current (0.1mA/div)
Zero is one division down the central crosshair.

Typical examples of the signal generator driving voltage, the anode High Voltage excitation produced by the power amplifier and the current flowing in the circuit are shown in Figure 2. Similar curves were observed along the whole range of the frequencies tested (1-1000 Hz). A slight distortion of the high voltage step is observed and this was somewhat amplified at the higher frequencies.

The analysis of these curves indicates that as expected the current is in phase with the excitation voltage.

In the upper stage of the step, the anode attains positive HV values and the voltage difference between the electrodes is high enough to enable the plasma sheet formation. The current flowing in the system exhibits a first peak, as consequence of the large displacement current (capacitive effect), followed by a relaxation process towards a quasi-steady value with small current peaks.

In a second phase, when the driving voltage is at the lower stage of the step the voltage of the anode vanishes. In this stage even though the cathode remains at high negative voltage the plasma sheet is no longer formed, and the current only exhibits a negative peak associated to a displacement current (capacitive effect) followed by a relaxation process.

Similar discharges to the one observed have previously received different denominations as skimming, grazing, or sliding discharge. Main aspects of it have been described under the theory of ionization waves[28].

In our experiments the discharge exhibits quite similar characteristics (such as luminosity, noise emission and sheet thickness) to the ones previously observed with DC excitation[25]. The steady excitation is probably a pulsating discharge consisting in a repetition of ionization waves. The resident space charge produced in each ionization wave, screens the external imposed electric field and impedes the formation of a new front of ionization until their neutralization. Recent experimental results have given further insight of this aspect[29].

Frequency of excitation of the actuator and frequency of actuation

The frequencies of excitation of the actuator considered in this work spanned form 1-1000 Hz while the reduced frequencies have been in the range $0.008<F^{+}<17$.

As a consequence of the discharge characteristics, the actuation occurs in the interelectrode region forcing the fluid layers at close vicinity of the surface. It has not still been demonstrated the coincidence between the frequency of the forcing on these layers agrees and the frequency of the electric excitation of the actuator. This has not been studied in this report but is subject of present research[30] .

B. Surface Pressure Distributions and Time averaged flow fields

The results of the mean pressure distributions and of the time averaged flow fields were analysed in the absence or in the presence of the actuation for different frequencies of excitation. The pressure distribution corresponding to a theoretical inviscid flow obtained from the formulation of Theoderse is used as a reference for the analysis of the experimental results [31]. The results of the time averaged velocity fields are in all cases illustrated with the streamlines corresponding to these averaged fields.

We have observed different flow behaviors as a consequence of the actuation, and we have gathered them in three groups or regimes: near poststall, middle poststall and deep poststall regimes

Near Post stall regime:

In the near post stall regime (reduced angles of attack) a complete flow reattachment may be achieved by a suitable actuation. The reattachment may be achieved either adjusting the power supplied by the actuator to the flow or by adjusting the frequencies of excitation.

In Figure 3 a case for α=15.8º with a coefficient characterizing the relative power supplied to the flow Cw=80.2 10^{-3} is represented. In this case the unforced flow exhibits a large plateau on the suction side of the airfoil that is

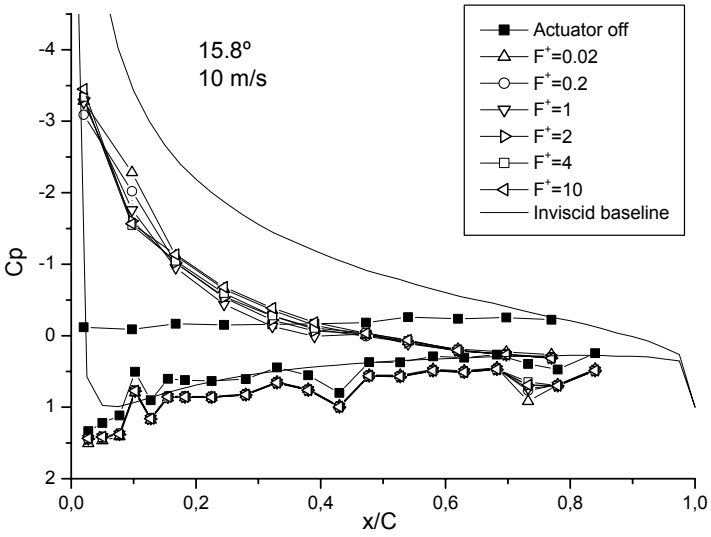

Figure 3: Near Post stall Regime Surface Pressure Distribution.
Angle of attack 15.8º, Re= 133333, C_W= 80.2 10^{-3}.

characteristic of a fully separated flow. The actuation originates the plateau producing elimination with a strong low pressure region near the leading edge followed by a rapid pressure recovery towards the trailing edge. The adjustment of the frequency of excitation may alter the pressure distributions on the suction side in the interelectrode space but the pressure recovery towards the trailing edge is similar for all the frequencies considered. In consequence the extrados pressure distributions agree with fully attached flow distributions independently of the frequency considered.

On the intrados the actuation increases in all points the value of the pressure indicating a decrease of the flow velocity in this side. Downstream the airfoil, when separation takes place the deficits of velocity of the wake produce an important deficit of mass flow in the wind tunnel section. To satisfy the mass conservation equation, the flow must compensate such deficit with an increase of the velocity in different regions including those of the intrados. When the flow becomes fully (or partially) reattached the wake disappears (or diminishes its wideness) and the regions of irrotational flow are not (or less) forced to compensate the deficit in mass flow. A reduction of velocity of the intrados, as we observe when the flow is forced, is in consequence consistent with the reattachment phenomenon.

The intrados pressure shows no clear influence of the frequency of excitation in agreement with the occurrence of full flow reattachment regardless of the frequency of excitation.

The time averaged flow fields and the streamlines of this averaged field are represented in Figure 4 and are a useful tool to better illustrate our analysis. In absence of actuation the existence of a clear recirculation zone

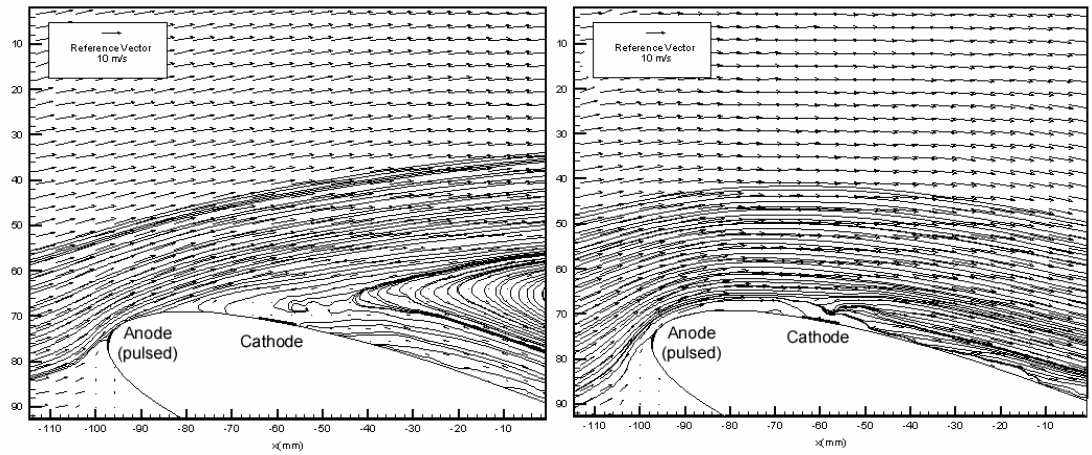

Figure 4: Near Post stall Regime Time averaged flow fields.
Angle of attack 15.8º, Re= 133333
Figure 4a (at left): Actuator off- C_W =0.0
Figure 4b (at right): Actuator on, C_W=80.2 10^{-3}, F^+ = 1

associated to the separated flow can be observed in figure 4a. Under the actuator operation (Figure 4b) such zone disappears at the time a reattachment of the flow takes place. Although within regions close to the downstream electrode, a slight deformation associated to PIV results contamination may appear, the streamlines contouring the model indicates a full flow reattachment. Such contamination may be due to illumination problems produced by a reflex of the laser sheet on the electrode.

In Figure 5 and Figure 6 there are represented cases of the near stall regime at higher angle of attack (α=19.8º) with *Cw* coefficients about one order of magnitude lesser than those of the preceding set of experiments.

In Figure 5a (C_W=4.9 10^{-3}) for nearly every curve representing the surface pressure with actuation, it is observed a low-pressure region near the leading edge on the suction side of the airflow followed by a small pressure recovery towards the trailing edge. The bubble of separation indicated by the presence of a plateau of pressure occupies a position close to the trailing edge and does not cover the whole upper surface as it does in the absence of discharge.

In concordance with results obtained with other actuators (v.g. Weier[22]), the size of this bubble may be reduced to almost its disappearance by adjusting either the frequency or the power supplied to the flow.

For the same level of power of actuation, it can be observed in Figure 5a that the curve corresponding to $F^+ \approx 0.4$ outstands from the rest. For this frequency the pressure recovery towards the trailing edge is more important and in consequence the bubble suffers an important reduction of its size.

On the other hand, Figure 5b (C_W=9.3 10^{-3}) demonstrates that for the same angle of attack (α=19.8º), an increase in power leads to a pressure distribution which indicates that separation is largely postponed.

In both cases of Figure 5, the actuation produces an increase of the pressure in the intrados, rersembling the curves to those corresponding with the inviscid pressure distribution. One more time this occurs regardless of the frequency of excitation as the bubble of the actuated flow, of slight size in all cases, only produce reduced velocity deficits.

The corresponding time averaged flow field velocities and the associated streamlines are represented in Figures 6 and in Figures 7.

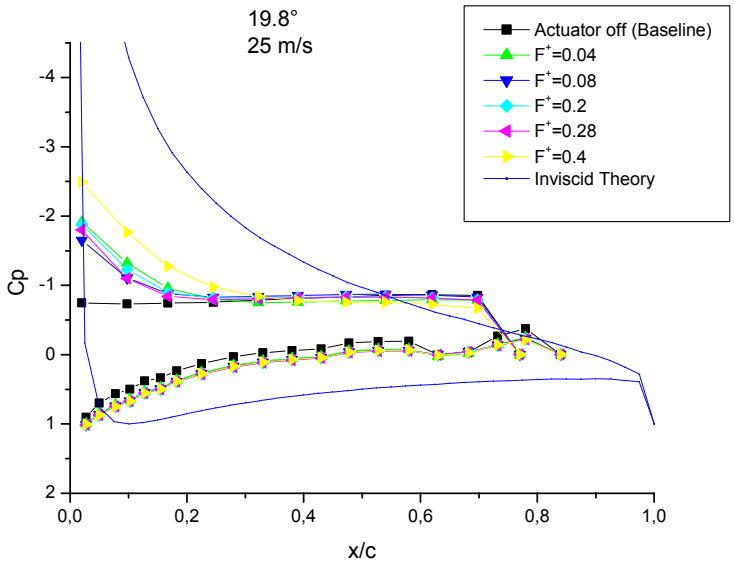

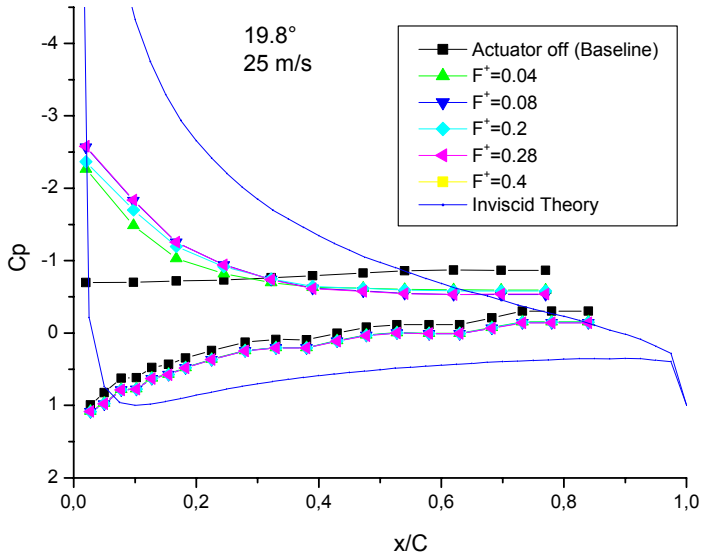

Figure 5: Near Post stall Regime Surface Pressure Distribution.
Angle of attack 19.8º, Re= 333333,
Figure 5a (top): $C_W=4.9\ 10^{-3}$
Figure 5b (bottom): $C_W=9.3\ 10^{-3}$

The flow without actuation (Figure 6a) exhibits a large bubble of recirculation associated with the flow separation. As a consequence of actuation with a moderate Cw (Figure 6b) a partial reattachment can be obtained meanwhile a large bubble transforms to one with a smaller size located in a position quite close to the trailing edge.

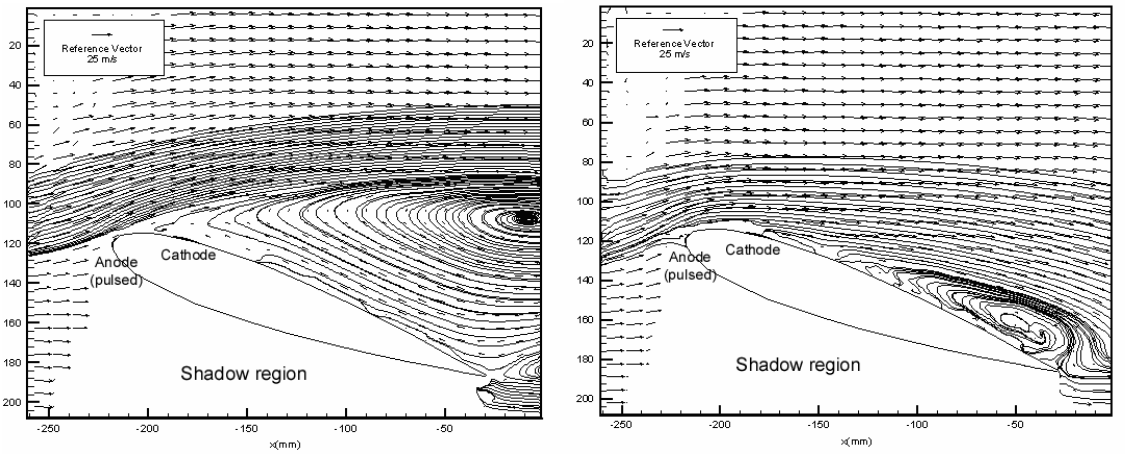

Figure 6 : Near Post stall Regime Time averaged flow fields with associated streamlines.
Angle of attack 19.8º, Re= 333.000
Figure 6a (at left): Actuator off-W=0.0
Figure 6b (at right): Actuator on, $C_W=4.9\ 10^{-3}$, $F^+=0.28$
(Laser sheet of PIV does not penetrate in the shadow region)

For the same Cw, and adjusting the frequency of excitation (Figure 7a) the reattachment process can be enhanced. Effectively, this figure demonstrate that the recirculation bubbles may fully or almost fully disappear producing a reattachment of the flow, with no clear recirculation bubble present.

On the other hand by increasing Cw the size of the recirculation bubble can be largely diminished (Figure 7b). A comparison of Figures 7a and 7b indicates however that the attachment is better with frequencies adjustment (almost full reattachment) than by power increasing (partial reattachment with a small bubble in the trailing edge).

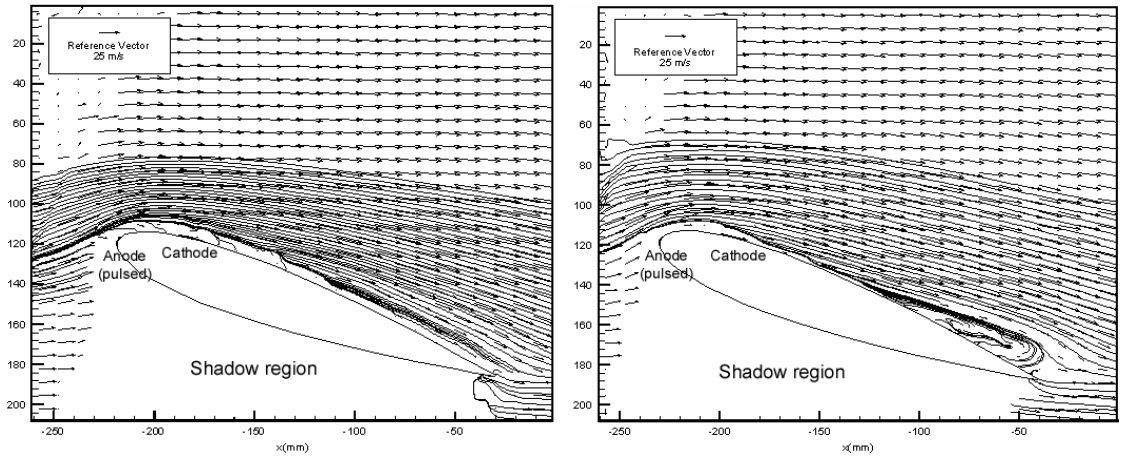

Figure 7: Near Post stall Regime Time averaged flow fields with associated streamlines.
Angle of attack 19.8º, Re= 333333
Figure 7a (at left): Actuator on, $C_W=4.9\ 10^{-3}$, $F^+=0.40$
Figure 7b (at right): Actuator on, $C_W=9.3\ 10^{-3}$, $F^+=0.28$
(Laser sheet of PIV does not penetrate in the shadow region)

Middle post stall regime

The separated flow became more sensitive to the effect of periodic excitation when the angle of attack was increased. Fig. 8 brings out the difference of behavior with the preceding cases. The figure reveals that a frequency adjustment towards the lower range produced higher values of pressure in the intrados where curves showed a more marked trend to the inviscid behavior; in association with a reduction of the deficit of velocity downstream the body.

The adjustment of the value of the frequency also produced changes in the extrados pressure distribution. Excitations in the low frequency range produced a pressure recovery on this side in agreement with a extensively attached flow. However, for the high frequencies range the actuator resulted less effective to improve the recovery of the pressure towards the trailing edge.

The time averaged flow fields and their associated streamlines are shown in Figure 9. The recirculation bubble

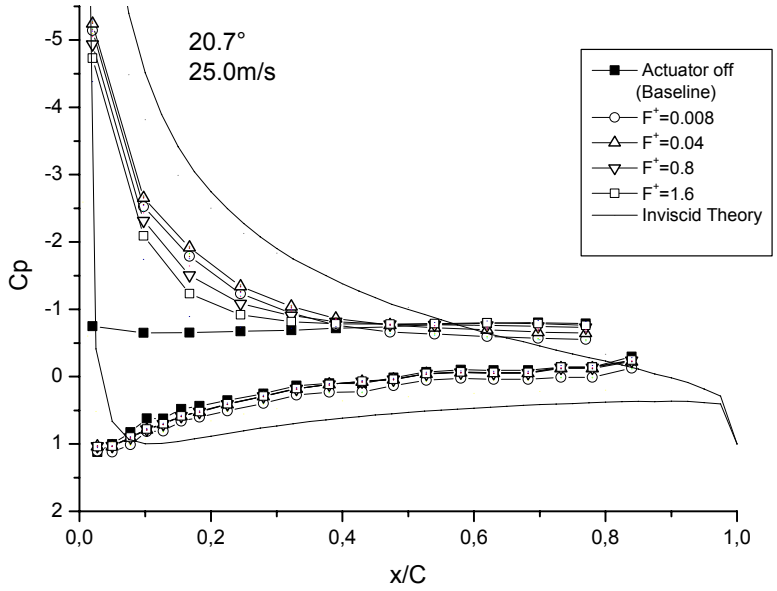

Figure 8: Middle Post stall Regime Surface Pressure Distribution.
Angle of attack 20.7º, Re= 333333, C_W=8.9 10^{-3}

clearly established without actuation (Figure 9a) disappeared when the actuator was applied (Figure 9b) exept for a perturbed zone in the region close to the downstream electrode. The flow contoured this perturbed region, in some sense similar to a separation bubble, and reattached downstream. As the frequency of excitation is increased the size of this zone became more ample. However this size modification did not produce an alteration of the flow detectable by the pressure distribution tests.

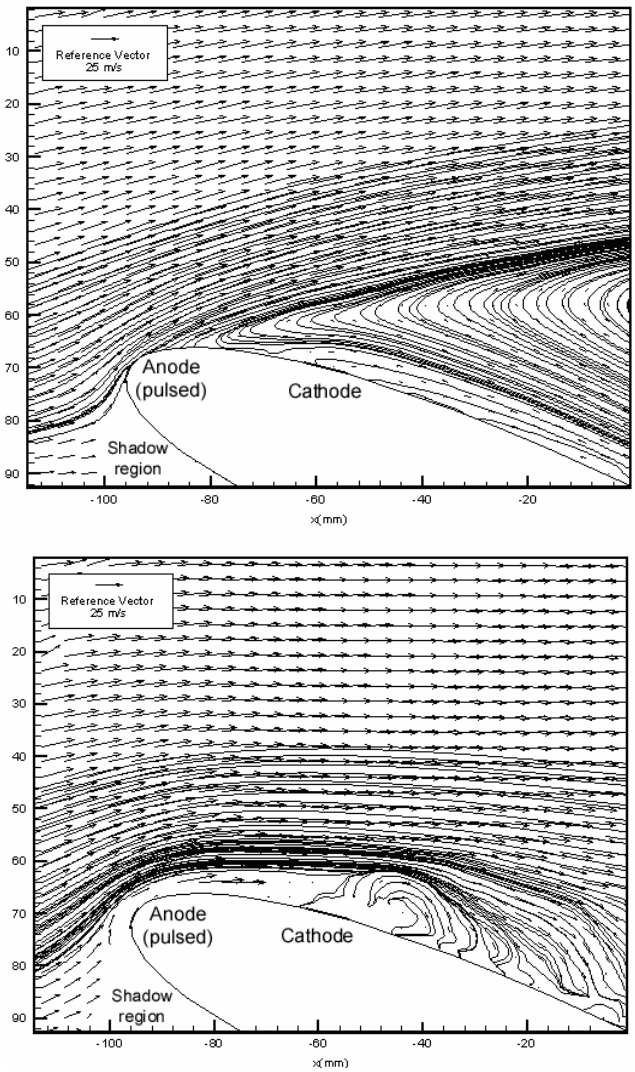

Figure 9: Middle Post stall Regime Time averaged flow fields with associated streamlines.
Angle of attack 20.7º, Re= 333333
Figure 9a (top): Actuator off, $C_W=0.0$
Figure 9b (bottom): Actuator on, $C_W=8.9\ 10^{-3}$, $F^+=0.28$
(Laser sheet of PIV does not penetrate in the shadow region)

Deep post stall regime

At higher values of the attack angle a deep stall regime occured. In this regime the flow could not be forced to a fully reattached configuration neither by increasing C_W nor by modifying the frequencies of excitation of the actuator.

Figure 10 illustrates the fact that even using higher values of C_W than in the preceding cases ($C_W=11.1\ 10^{-3}$) a full reattachment could not be achieved for any tested frequency. Effectively, regardless of the frequency considered the extrados pressure distributions exhibited a low-pressure region near the leading edge followed by a large plateau associated to a bubble of separation at positions close to the leading edge.

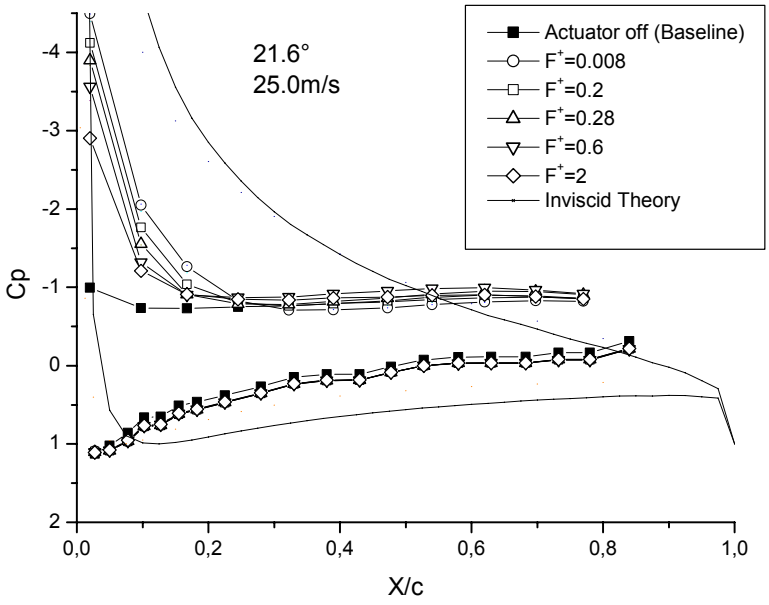

Figure 10: Deep Post stall Regime Surface Pressure Distribution.
Angle of attack 21.6º, Re= 333333, C_W=11.1 10^{-3}

The maximum suction peak, the pressure value of the plateau and the position starting of the plateau where modified upon a frequency variation. These parameters changes reflected into modifications of the size of the separation bubble
Then, even though the EHD forcing only permitted to partially reattach the flow, a control of the separation line in this regime may still be achieved by adjusting the value of the frequency of excitation .

The time averaged flow fields and their associated streamlines are shown in Figures 11 to better illustrate the pressure distribution results. There exists a large bubble when actuation is off while, a reduction and displacement of the bubble towards the trailing edge occurs when the actuation is on.
The PIV tests for this regime, in concordantly with the pressure tests, have also revealed that the size of the recirculation bubble and its position depended on the frequency of excitation. Our observations indicate that the larger bubbles are produced as the frequency of excitation reaches the higher values.

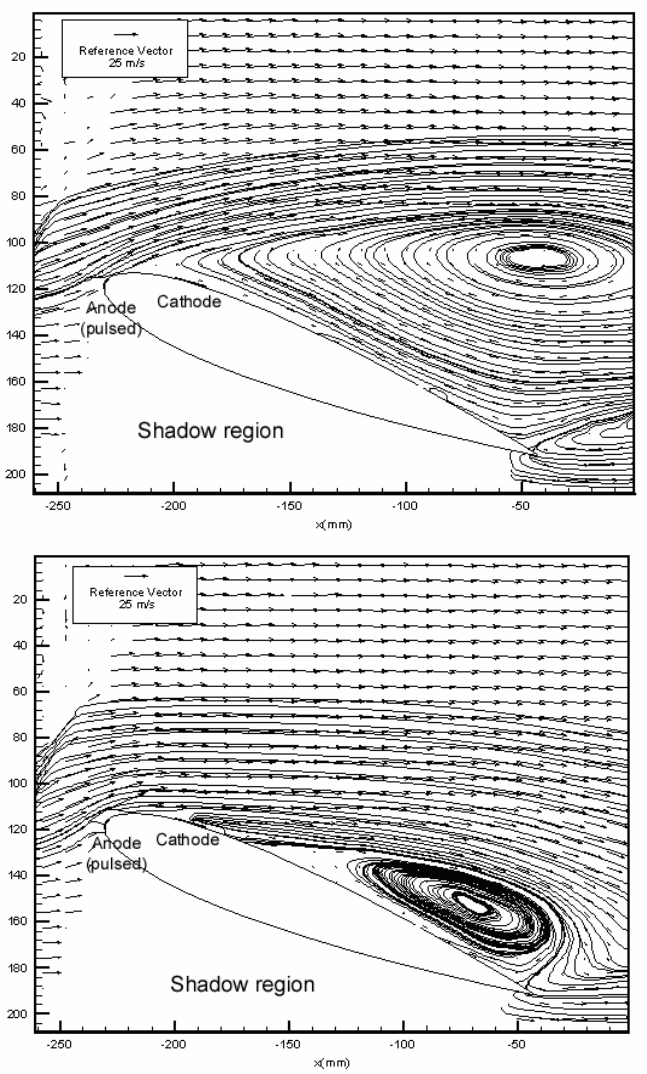

Figure 11: Deep Post stall Regime Time averaged flow fields and associated streamlines.
Angle of attack 21.6º, Re= 333333
Figure 10a (top): Actuator off, $C_W=0.0$
Figure 10b (bottom): Actuator on, $C_W=11.1\ 10^{-3}$, $F^+=0.08$
(Laser sheet of PIV does not penetrate in the shadow region)

C. Lift and drag pressure coefficients

Once demonstrated that for the different angles of attack there exists an influence of the reduced frequency on the reattachment process, the analysis of its effects on the lift and drag pressure coefficients would enable, in some extent, to better highlight this dependency.

Figure 12 analyses the lift coefficient differences ΔC_l (actuation on minus actuation off) and of the difference of the ratio $\Delta(C_l/C_{Dp})$ (actuation on minus actuation off) as a function of reduced frequencies. The values of the C_l and C_{Dp} coefficients for the non actuated case for different angles of attack are detailed in Figure 12 caption.

A comparison of the reported values with those corresponding to a DC excitation may also be carried out considering our previous results[19] reproduced in table II. This analysis enables a global comparison of the effectiveness of steady and periodic excitation of the flow.

Near post stall regime

For this regime the influence of the frequencies of excitation on the aerodynamic coefficients may be deducted from the curves for α=15.8º and α=19.8º in Figure 12.

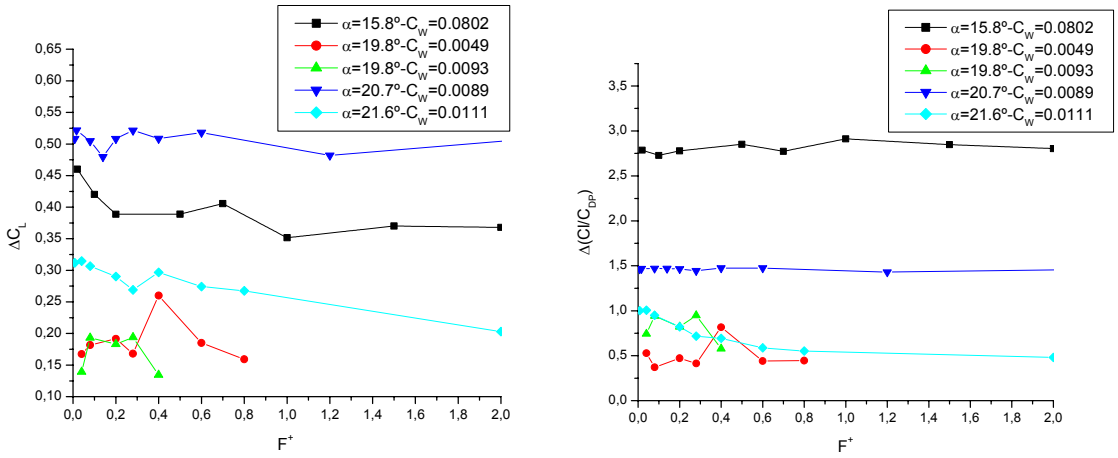

For the case with the lowest angle of attack (α=15.8º) an important increase of the aerodynamic coefficients C_l and of the ratio C_l/C_{Dp} has observed, as a consequence of actuation. These enhancement was associated, as previously detailed, to the passage from a fully separated flow (actuator off) to a fully attached flow (actuator on).

The better performance of the lift coefficient C_l was achieved at the low range of frequencies F^+, range in which the largest values of suctions in the interelectrode region were observed. However the lack of a clear effect of the frequency of excitation on the ratio C_l/C_{Dp} indicated a compensation of the lift coefficient increase with a simultaneous drag pressure increase when the flow around the airfoil inhibited no separation.

Comparison of this case with the steady excitation experiments indicated that similar airfoil performances may be achieved by adjusting the power of the DC actuator, however DC actuation require to supply a larger power to the flow.

At higher angles of this regime and for reduced values of power (curves for α=19.8º- $Cw=4.9\ 10^{-3}$) a peak in the actuated airfoil performance coefficient occurs in correspondence with $F^+\approx0.4$, a value for which a full or almost full reattachment has been observed. With other frequencies the flow exhibits a bubble of recirculation that depending on its size degradates more or less the airfoil performance.

For the same angle of attack and as power is increased (curves for α=19.8º- $Cw=9.3\ 10^{-3}$ of Figure 12a) the lift coefficient may attain similar values than those of the preceding case meanwhile the ratio Cl/C_{Dp} is higher. This last may be ascribed to the important incidence on the pressure drag of the bubble size. Figure 6 and 7 reveal that actuation with larger power produces bubble size shorter than those of the lower power in the non-optimized frequency case. A reduction of C_{Dp} and an improvement of the ratio Cl/C_{Dp} should in consequence occur as we observe in Figure 12.

For this angle of attack, a comparison of the steady and periodic excitation (Table II) indicates that DC excitation may achieve similar or better effects than those of periodic but it requires larger power consumption.

α (º)	C_W	ΔCl	$\Delta(Cl/C_{Dp})$
15.8	0,162	0.42	2.75
15.8	0,306	0.43	2.80
15.8	0,388	0.45	3.15
19.8	0.022	0.29	1.28
19.8	0.042	0.52	1.68
20.7	0,017	0.08	0.33
20.7	0,026	0.13	0.44
20.7	0,036	0.19	0.69
20.7	0,047	0.28	0.84
21.7	0.033	0.35	0.97

Table II: Difference on coefficients of aerodynamic performance as a consequence of actuation with a DC excitation (reproduced from [19])

For the cases actuator off the coefficients Cl and the ratio Cl/C_{Dp} are the same of the caption of Figure 12.

Middle Post stall regime

The behavior in this regime is illustrated in Figure 12 by the curves for the angle of attack α=20.7º.

In this regime it has been observed a flow situation with a perturbed region in the proximity of the surface (separation bubble) followed by a reattachment of the flow when actuation is operated.

The size of the bubble increases as frequency of the excitation approaches the higher values but a degradation of the airfoil performance is not clearly observed for this range of frequency. The detrimental effect of this bubble is quite reduced probably as a consequence that downstream the bubble there exists a reattachment of the flow and also because the periodic excitations finally give rise to bubbles with a small size. The curves corresponding to this regime can be observed from the Figure 12, and the curves for this regime show similar behaviours to the ones corresponding for α=15.8º (case with full reattachment)

A comparison with steady excitation clarifies however, the sensitivity of this regime to periodic excitation. The values of Table II indicate that the same performance of the airfoil may not be achieved by steady excitation even supplying values of power one order of magnitude larger than the one supplied in the periodic excitation tests. The sizes attained by the bubbles on the actuated flow with steady excitation are in fact significant enough to diminish the airfoil performance.

Deep post stall regime

At these regimes the flow is partially reattached and it can be observed a degradation of the airfoil performance as higher values of frequencies are used. This is ascribed again to the influence of the frequency of excitation on the size and position of the recirculation bubble. As the lower frequencies better postpone the separation than the higher frequencies, the airfoil performance enhances for these frequencies.

The comparison with steady excitation indicates that in this regime similar effects may be achieved by the DC actuator by suitable adjusting the power of it, but also occurs that this actuation as in the near stall regime require large power supply to reattach the flow

IV. Conclusions

We show in this article that with a periodic actuation provided by an EHD actuator it is possible to prevent or postpone stall in an airfoil.

According to the angle of attack and to the receptivity of the flow to the dynamic actuation three different groups could be identified: near, middle and deep post stall regime. In the first regime a full or almost full reattachment of the flow may be achieved either by a suitable adjustment of the frequency of excitation or of the power supplied to the actuator. In the middle post stall regime, the actuation gives rise to a flow configuration with a recirculation bubble followed by reattachment. For the third group only a partial reattachment could be observed

In general, for the three groups at a fixed value of power the high frequency range ($F^+>2$) proofed to be less effective to improve the aerodynamic performance of the airfoil than the low range ($F^+<1$).

A comparison of steady excitations with periodic ones indicate that similar effects could be achieved in the first and third group, but the steady excitation required large power consumption. However, in the middle post stall regime the aerodynamic performance of the airfoil obtained with periodic excitation could not be achieved by steady actuation at any power.

These results encourage the study of periodic excitation as a mean of improving efficiency in actuation with EHD in flows with separation.

Acknowledgments

This research has been done with grants UBACYT I003 and PICT 12-09482 of the Argentine government. We thank the University of Poitiers for inviting Prof. G. Artana to the Laboratoire d'Etudes Aerodynamiques during January and February of 2003 when experiments were performed.

V. References

[1]. J D'adamo; G. Artana, E. Moreau, G. Touchard, "Control of the airflow close to a flat plate with electrohydrodynamic actuators", ASME Paper Nº 2002-31041.

[2] Bushnell D., "Turbulent Drag Reduction for External Flows", AIAA paper N° 83-0227.

[3] Malik M., Weinstein L., Hussaini M., "Ion Wind Drag Reduction", AIAA paper N° 83-0231.

[4] Colver G., El-Khabiry S.,. "Modeling of DC Corona Discharge Along an Electrically Conductive Flat Plate with Gas Flow", *IEEE Trans on Industry Appl.,* Vol. 35, No. 2, 1999, pp. 387-394.

[5] Noger C., Chang J. S., Touchard G., "Active Controls of Electrohydrodynamically Induced Secondary Flow in Corona Discharge Reactor" Proc. 2nd Int'l Symp Plasma Techn. Polution Cont, Bahia, pp.136-141, 1997

[6] Roth J. R. and Sherman D. "Electrohydrodynamic flow control with a glow discharge surface plasma", *AIAA J.* , Vol 38 , No 7, , 2000, pp 1166-1178.

[7] Wilkinson S. P. , "Investigation of an Oscillating Surface Plasma for Turbulent Drag Reduction",. AIAA Paper Nº 2003-1023.

[8] E. Kunhardt, Generation of large volume atmospheric pressure non –equilibrium plasmas, *IEEE Transactions on Instrumentation and measurements*, 28(1), 2000, pp 189-200.

[9] Huerre P. and Monkewitz P. "Local and global instabilities in spatially developing flows", *Annu. Rev. Fluid Mech*. 22, 1990, pp 473-537.

[10] D. Greenblatt, I. Wygnanski, "The control of flow separation by periodic excitation", *Progr. Aerosp. Sci.,* 36, 2000, pp 487-545.

[11] I. Wygnanski, "Boundary layer and flow control by periodic addition of momentum", AIAA paper Nº 97-2117

[12] Johnson J. and Scott S. , "Plasma-Aerodynamic Boundary Layer Interaction Studies". AIAA paper Nº 2001-0523.

[13] Scherbakov Y. et al , "Drag Reduction by Ac Streamer Corona Discharges along a wing-like profile plate", AIAA paper Nº 2000-2670.

[14] Corke T., Jumper E., Post M., Orlov D. and McLaughlin T. , " Applications weakly ionized plasmas as wing flow control devices", AIAA Paper Nº 2002-0350.

[15] Post M., Corke T., "Separation control on high angle of attack airfoil using plasma actuators", AIAA Paper Nº 2003-1024

[16] Vilela Mendes R., Dente J., "Boundary Layer Control by Electric Fields", *Journal of Fluid Engineering*, Vol. 120, 1998, pp. 626-629.

[17] R. Sosa, Control de escurrimientos alrededor de perfiles alares con actuadotes EHD, Tesis de Grado, FIUBA, 2002 (in spanish)

[18] R. Sosa, G. Artana, Control del flujo alrededor de perfiles alares mediante el uso de actuadores EHD, *Escola de Transicao e Turbulence*, Florianopolis, [CD ROM], 2002. (in spanish)

[19]G. Artana, R. Sosa, E. Moreau, G. Touchard, "Stall control of airfoils at high angle of attack with EHD actuators steadily excited" (submitted for publication)

[20] M. Post, T. Corke, "Separation control using plasma actuators-stationary and oscillating airfoils", AIAA paper Nº 2004-0841.

[21] A. Seifert, A. Darabi, I. Wygnanski, "Delay of airfoil stall by periodic excitation", *Journal of Aircraft*, 33 (4), 1996, pp 691-698.

[22] Weier T. Gerbeth G., "Control of separated flows by time periodic Lorentz Forces", (Submitted to European Journal of Mechanics B/Fluids).

[23] G. Artana; R: Sosa, E: Moreau; G: Touchard, "Control of the near wake flow around a circular cylinder with electrohydrodynamic actuators*"*, *Experiments in Fluids* , 36 (6), 2003, pp 580-588.

[24] R. Keane, Adrian R., "Theory of Cross Correlation Analysis of PIV Images", *Applied Scientific Research*, Vol. 49, 1992, pp. 191-215.

[25] G. Artana, J. D'adamo, L. Leger, E. Moreau, G. Touchard, Flow control with electrohydrodynamic actuators, *AIAA Journal*, 40(9), 2002, pp 1773-1779.

[26] H. Bergh, H. Tijdeman, "Theoretical and experimental results for the dynamic response of pressure measuring systems", National Aero and Astronautical Research Institute, Amsterdam, NLR report F.238, 1965

[27] A. Roshko, "On the drag and shedding frequencies of two dimensional bluff bodies", NACA TM 3169, 61, 118, 1954

[28] Lagarkov A., Rutkevich I., "Ioniztion Waves in Electrical Breakdown of Gases", Springer-Verlag, NY, 1993, pp. 195-207.

[29] E. Moreau, G. Artana, G. Touchard , "Surface corona discharge along an insulating flat plate in air applied to electrohydrodynamically airflow control : electrical properties", Electrostatics'03, IOP Publishing Ltd, Bristol-Philadelphia. (in press)

[30] E. Moreau, A. Labergue, G. Touchard, "DC And Pulsed Surface Corona Discharge Along A PMMA Flat Plate In Air: Electrical Properties And Discharge-Induced Ionic Wind", 4th Intnl Symposium on Non thermal Plasmas for Pollution Control and sustainable Energy development, Panama city , Florida, 2004.

[31] T. Theodersen, "General potential theory of arbitrary wing sections", NACA Report #452, 1934.